

Design Optimization Using Numerical Simulation and Experimental of Wind Energy Harvester Unit from Exhaust Fan

By:

MUHAMMAD ZIKRI BIN ADNAN

(Matrix no. : 128960)

Supervisor:

Ir. Dr. Chan Keng Wai

29 May 2019

This dissertation is submitted to

Universiti Sains Malaysia

As partial fulfillment of the requirement to graduate with honors degree in

BACHELOR OF MECHANICAL ENGINEERING



School of Mechanical Engineering

Engineering Campus

Universiti Sains Malaysia

DECLARATION

It is declared that the content of the thesis report titled “Design Optimization Using Numerical Simulation and Experimental of Wind Energy Harvester Unit from Exhaust Fan” has been solely prepared by me, Muhammad Zikri bin Adnan under supervision of Ir. Dr. Chan Keng Wai. It is further declared that this is my original works, as part of the requirement for the course named EMD452 Final Year Project for Mechanical Engineering Degree at the School of Mechanical Engineering, Universiti Sains Malaysia.

Name: Muhammad Zikri bin Adnan

Matrix No.:128960

Date:

Name:

Date:

ACKNOWLEDGEMENT

Great thanks to Allah with His allowance for me to complete this final year project successfully. Thank you to my family members, for always having my back supporting me through this year. Not to forget my fellow friends who helped me to ease my journey while completing their project at the same time. On the university side, I would like to express my gratitude towards my supervisor, Ir. Dr. Chan Keng Wai for his guidance and help in accomplishment of this final year project and his joyful lectures along my study. Besides that, thanks to all university staff in administration, academic and technical assistant for prepare anything that I need to complete my project.

TABLE OF CONTENTS

ACKNOWLEDGEMENT	iii
TABLE OF CONTENTS	iv
LIST OF TABLES	vi
LIST OF FIGURES	vii
LIST OF ABBREVIATIONS AND SYMBOLS	ix
ABSTRACT (BM)	x
ABSTRACT (BI)	xi
CHAPTER 1: INTRODUCTION	1
1.1 Research Background	2
1.2 Problem Statement	3
1.3 Objective(s).....	3
1.4 Scope of Research	4
CHAPTER 2: LITERATURE REVIEW	5
2.1 Introduction	5
2.2 Comparison of Performance between Two Propulsion Mechanisms	5
2.3 Vertical Axis Wind Turbine (VAWT)	6
2.4 Effect of the turbine radius, wind speed, shroud exit area to turbine area ratio and shroud exit length to the power generated and power coefficient	8
CHAPTER 3: METHODOLOGY	14
3.1 Design of Energy Harvester Unit.....	14
3.1.1 Design of Curve Duct	14
3.1.2 Design of Nozzle and Diffuser	17
3.1.3 Design of Generator Unit	20

LIST OF TABLES

Table 2.1: Two mechanisms of propulsion compared.

Table 2.4.1: Parameters of thirteen computed cases.

Table 2.4.2: Power production and power coefficient C_p for thirteen cases of 1(a).

Table 3.1.1.1: Various design configuration of the curve duct.

Table 3.1.1.2: Design model of the curve duct with different parameters configuration.

Table 3.1.2.1: Design parameter of the various nozzle and diffuser configuration.

Table 3.1.2.2: Solidworks design of the nozzle and diffuser with different parameters configuration.

Table 3.1.3.1.1: Design parameter for NACA4412.

Table 4.1.1: Numerical simulation result of various curve duct design configuration.

Table 4.1.2: Simulation result of the curve duct A, B, C and D

Table 4.1.3: Numerical simulation result of the nozzle and diffuser with various design configuration.

Table 4.1.4: The simulation result of air velocity at point 1, 2, 3, 4 and 5.

Table 4.1.5: The experimental result of air velocity at point 1, 2, 3, 4 and 5.

Table 4.1.6: Comparison of simulation and experiment result with percentage error.

Table 4.1.7: Parameter value for model and real size energy harvester unit.

LIST OF FIGURES

Figure 1.1: Fuel consumption in electricity generation in Malaysia.

Figure 2.2.: The velocity profile bands of the cooling tower air outlet.

Figure 2.3.1: Complete scale model of VAWT on cooling tower.

Figure 2.4.1: Schematic of axisymmetric HAWT actuator disk model and shroud parameters.

Figure 2.4.2 (a): Mesh inside the shroud for case 1(a)

Figure 2.4.2 (b): Total pressure inside the shroud for case 1(a).

Figure 2.4.3 (a): Static pressure contours inside the shroud for case 1(a).

Figure 2.4.3 (b): Velocity magnitude contours inside the shroud for case 1(a).

Figure 2.4.4 (a): Velocity variation along the centre of the shroud for case 1(a).

Figure 2.4.4 (b): Static pressure variation along the line of axis the shroud for case 1(a).

Figure 2.4.5: Total pressure variation along the axis of the shroud for case 1(a)

Figure 2.4.6: Thirteen optimized diffuser shapes for thirteen cases in Table 1 for a 5 ft radius turbine (shown as an actuator disk).

Figure 3.1.2.1: Parameter guide of the nozzle and diffuser.

Figure 3.1.3.1.1: Parameter guide of an airfoil.

Figure 3.1.3.1.2: Cross-sectional design of NACA 4412 airfoil based on the coordinated grid.

Figure 3.1.3.1.3: $\frac{C_L}{C_D}$ relationship of NACA 4412.

Figure 3.1.3.1.4: Lift coefficient against angle of attack of NACA 4412.

Figure 3.2.1(a): Side view of the structured mesh grid of curve duct design B with 1.41 m of turning radius. (b): structured mesh grid of the duct inlet.

Figure 3.2.2: Isometric view of full model with vortex generator used for simulation.

Figure 3.2.3: Side view of the full model with dimension in centimetre.

Figure 3.3.1.1: CAD model in isometric view of the curve duct.

Figure 3.3.1.2: CAD model of NACA 4412 turbine blade.

Figure 3.3.1.3: CAD model of the complete wind turbine assembly.

Figure 3.3.1.4: Material Properties of ABS.

Figure 3.3.1.5: 3D printed wind turbine by using ABS material.

Figure 3.3.1.6: 3D printed curve duct by using ABS material.

Figure 3.3.2.1: Isometric view of CAD model of combined nozzle and diffuser.

Figure 3.4.1: Open circuit wind tunnel located in School of Aerospace Engineering laboratory.

Figure 3.4.2: Experiment set up on an open circuit wind tunnel located in school of aerospace engineering laboratory.

Figure 4.1.1: Air velocity distribution along the ducting.

Figure 4.1.2: Air pressure distribution along the ducting.

Figure 4.1.3: Graph of simulation and experiment result.

Figure 4.1.4 (a): Simulation result of air flow through the ducting. (Front view)

Figure 4.1.4 (b): Simulation result of air flow through the ducting. (Side view)

LIST OF ABBREVIATIONS AND SYMBOLS

P_w Power extracted from wind

ρ Air density

A Cross-sectional area

v Air velocity

L Lift Force

D Drag Force

C_L Lift coefficient

C_D Drag coefficient

R Turning radius

β Blade setting angle.

C Chord length

α angle of attack

S Particle path line

r Radius

\angle Angle

NACA National Advisory Committee for Aeronautics

W Watt

HP Horsepower

T Torque

ABSTRACT (BM)

Keperluan sumber tenaga yang boleh diperbaharui dan mampan semakin meningkat kerana sumber-sumber semula jadi yang semakin berkurangan di seluruh dunia. Cara lama yang digunakan untuk menjana elektrik semakin lenyap dan akan digantikan dengan sistem penukaran tenaga yang boleh diperbaharui dan mampan. Kaedah baru dijangka menghasilkan kurang pelepasbahan yang berbahaya kepada manusia dan alam sekitar dengan kecekapan yang lebih tinggi. Oleh itu, penggunaan konsep kincir angin adalah satu daripada penyelesaian utama untuk menjana elektrik untuk kegunaan domestik dan industri. Dengan potensi tenaga kinetik tinggi yang kenal pasti di salah sebuah pengeluar tekstil di Perai, menggunakan unit penuai tenaga dengan konsep kincir angin telah saya cadangkan untuk menuai tenaga yang terbuang dan mengubahnya menjadi tenaga elektrik yang berguna. Tenaga elektrik yang dihasilkan dijangka akan digunakan oleh Penfabric Mill 2 sendiri sebagai salah satu langkah ke arah penerapan teknologi hijau dalam industri penghasilan. Pengoptimuman telah dilakukan dengan menggunakan perisian simulasi berangka yang dinamakan ANSYS dan akan disahkan melalui eksperimen model berskala. Percubaan diadakan di makmal aeroangkasa di kampus kejuruteraan dengan menggunakan terowong angin litar terbuka untuk mensimulasi keadaan industri yang sebenar seperti di Penfabric Mill 2. Sebagai kesimpulan, reka bentuk saluran udara yang optimum dihasilkan dari kajian komputasi dan eksperimen ini.

ABSTRACT (BI)

The need of renewable and sustainable energy sources is increasing exponentially as the natural resources are depleting around the world. The old way of generating electricity are vanishing and will be replaced by new renewable and sustainable energy conversion system. New method are expected to produce less emission of dangerous substances for human and environment with higher efficiency. Therefore, the use of wind turbine concept is one of the key solution to generate electricity for domestic an industrial use. With the high potential of kinetic energy recognized in one of the textile manufacturer in Perai, the energy harvester units with the wind turbine concept was proposed to harvest the wasted energy and convert it into useful electrical energy. The produced electrical energy are expected to be used by the Penfabric Mill 2 itself as one of the move toward the green technology implementation in the manufacturing industry. Optimization were done by using numerical simulation software named ANSYS and will be validate through a scaled model experiment. The experiment are held in aerospace laboratory in engineering campus by using an open circuit wind tunnel to simulate the real industrial condition just like in Penfabric Mill 2. The same air flow pattern were obtained from the simulation and experiment result with slight different in value at each point. As a conclusion, an optimum air duct design was produced from this computational and experimental study.

CHAPTER 1

INTRODUCTION

Electric energy relate closely to the economic growth and development of a country. Electric power generation in Malaysia is highly depend on fossil fuel like coal, natural gas and fuel-oil. During the energy conversion, the burning of the fossil fuels produces greenhouse gases (GHGs). Greenhouse gases leads to environmental degradation and world climate changes.

Malaysia's effort to achieve the developed country status through sustainable development. Therefore, the development activities in Malaysia are required complying with all the component of sustainability namely economy, environment and society. Sustainable energy generation is the key of sustainable development, globally and nationally.

Alternative energy generator is what this project is going to introduce. Energy in the form of electricity can be generated from the wind energy. The exhaust wind energy is an industrial form of energy waste from the air-conditioning and ventilation system. A large manufacturer uses large air-condition system to control the temperature and humidity over the large production area. The larger the air-condition system, the larger the energy waste in form of wind energy produced. I believe that it may reduce the electricity generation cost, greenhouse gases emission, and lead to better sustainability of our country.

There are few researches have been made before, but mostly only focused on the energy harvesting from the cooling tower. They tried to design the energy harvester unit by using vertical axis wind turbine (VAWT). In this project, we will use horizontal axis wind turbine (HAWT) to harvest the wind energy from the air-condition exhaust fan. The design will be made based on the real industry constraint in Penfabric Mill 2 production site.

This project will focus on the design optimization through two method which are numerical simulation and experimental. At the end of this project, we are expected to obtain the high efficiency energy harvester unit design.

1.1 Research Background

The wind turbine application in Malaysia is limited due to the average natural wind velocity is below the minimum air flow velocity required to turn even a small wind turbine. Due to this factor, the energy generation in Malaysia is highly depend on the hydropower, diesel, fuel oil, coal and natural gas. Based on the study in 2015, about 64% electrical energy was used in peak hours by the industries and the average power factor ranged from 0.88 to 0.92.

Malaysia, being a developing country, we are expected to have continuous rise in energy demand. In last two decades, Malaysia's gross domestic production grew steadily at an average of 5.8% from 1990 to 2012. Malaysia's energy consumption grew on average of 6.62% from 1980 to 2012 [1].

The current electric generation methods have significant impact on country fuel consumption demand. Figure 1.1 prepared in the energy journal in 2015 show the fuel consumption trends in electricity generation, where we can clearly observe that the electricity generation structure has experience significant changes twice [1].

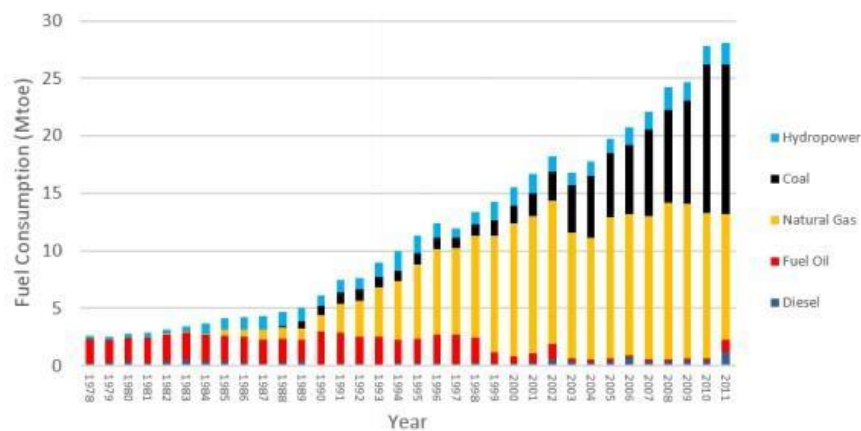


Figure 1.1: Fuel consumption in electricity generation in Malaysia.

The steady increasing trend indicate the increasing effect of the hazardous gases emission from fuel combustion will also increase. Therefore, the alternative way of electric generation is needed to reduce this bad impact.

Instead of relying on the low natural wind energy in Malaysia, an alternative way of harvesting wind energy is from the continuous wind producer. This large wind energy can be obtain from the large factory exhaust fan. The exhaust fan out flow will continuously create air flow as long as the factory operation are still running.

This project is concerning on one of the energy sources element which is wind energy. The proposed optimization will use the numerical simulation and experimental verification.

1.2 Problem Statement

Large waste energy in form of air flow in Penfabric Mill 2 production site at 18 – 20 m/s of maximum air velocity with average of 10-11m/s were recognized. The calculated wind power from one exhaust fan is 1044.009W every one second. The Penfabric Mill 2 operate at 24 hours per day, which will lead to 90.202 MW per day. With the 624 hours of operation per month, the energy that being wasted by 1 exhaust fan is 2345.262 MW per month. With the total of twelve operating exhaust fans, it wasted 28.143 GW of energy per month and 337.718 GW per year. The energy calculated above is based on the current condition (6th November 2018) without any future production expansion yet.

1.3 Objective(s)

The objectives of this study are:

1. To design and propose an optimum air duct design configuration to channel and increase the air velocity from exhaust fan.
2. To investigate computational and experimental study on performance of the energy harvester unit.

1.4 Scope of Research

This project involves design, design optimization, simulation, fabrication, experimentation, and result analysis at the final stage. Before the design stage, an industrial visit is required to obtain the actual data regarding the exhaust fan area when the energy harvester unit will be installed. Space is a critical factor to be consider

because the ready exhaust fan design and position cannot be change easily. Some data of the physical quantity if the exhaust fan and air flow are needed to design the energy harvesting unit based on the specification needed. The design area of concern consist of curve duct, converge duct, wind turbine section, and generator position inside the ducting.

The numerical investigation of the aerodynamic characteristics of the whole system will be execute with the 3D simulation to obtain the optimum design. The optimization of the design will focus on the air flow available power output. After the overall simulation part is done, the scale model design will be bring for the fabrication process before the experiment will be executed. The fabrication stage is subdivided into rapid prototyping of the wind turbine and machining of the duct model. The high precision of the production is crucial for the determination of the aerodynamic characteristics of the model. The model will be tested on the open circuit wind tunnel to obtain the aerodynamic performance of the model.

CHAPTER 2

LITERATURE REVIEW

2.1 Introduction

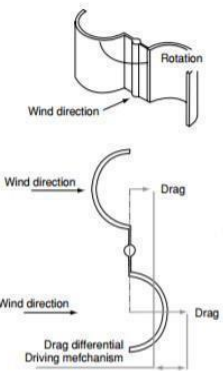
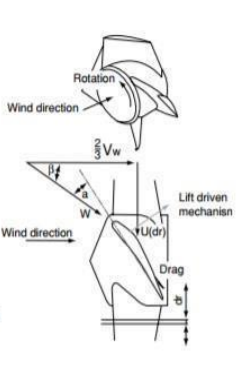
In this section based on the previous studies, the comparison of performance between two propulsion mechanisms of horizontal-axis wind turbines (HAWT) and vertical-axis wind turbines (VAWT) are described. The past research on the simulation of shrouded wind turbine are studied and their simulation method will be use as a guide for my study. As an output indicator, various parameter configuration are described as well to give the better idea to optimize the design through some of the system parameter.

2.2 Comparison of Performance between Two Propulsion Mechanisms

The commonly used wind turbines can be classified into two categories based on their rotate orientation, horizontal-axis wind turbines (HAWT) and vertical-axis wind turbines (VAWT). HAWT have their axis of rotation horizontal to ground and almost parallel to the wind stream. Most of the commercial wind turbines fall in this category. Likewise, the axis of rotation of VAWT is vertical to the ground and almost perpendicular to the wind direction.

Energy extracted from the wind turbine is extremely important in determining the maximum efficiency of the wind energy. Maximum achievable theoretical efficiency is highly depending on the method of propulsion [2]. Horizontal axis wind turbines have higher power efficiency than vertical axis wind turbines. Wind turbines that rely on drag force are insufficient power producers as their tip speed ration cannot exceed one. This is because the relative velocity of wind is reduced as the rotor speeds increases. The comparison of maximum theoretical efficiency is shown in Table 2.1.

Table 2.1: Two mechanisms of propulsion compared. [2]

Propulsion	Drag	Lift
Diagram		
Relative wind velocity	$= \text{Wind Velocity} - \text{Blade Velocity} = \sqrt{\frac{2}{3} \text{Wind Velocity}^2 + \text{blade Velocity}(dr)^2}$	
Maximum theoretical efficiency	16%[4]	50%[6]

2.3 Vertical Axis Wind Turbine (VAWT)

A research about energy harvesting from the cooling tower by using vertical axis wind turbine have been done in University of Malaya (UM). To avoid a negative impact on the performance of the cooling tower and to optimize the turbine performance, the determination of the VAWT position in the discharge wind stream was conducted by experiment.

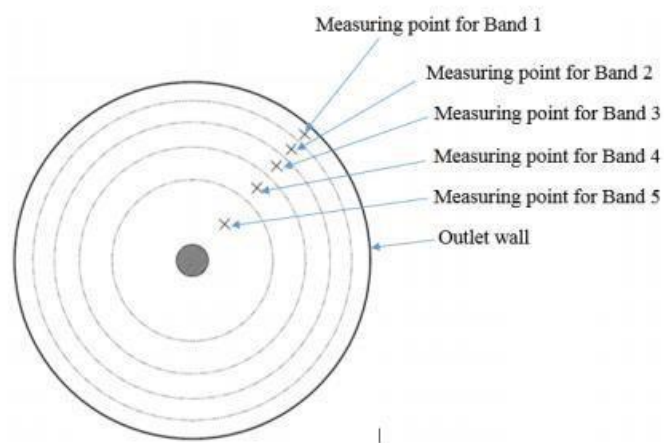


Figure 2.2.: The velocity profile bands of the cooling tower air outlet [3].

The preferable VAWT position is where the higher wind velocity matches the positive torque area of the turbine rotation. With the proper matching among the VAWT configurations (blade number, air foil type, operating tip-speed-ratio, etc.) and exhaust air profile, the turbine system also reduced the fan motor power consumption by 4.5% and increased the cooling tower intake air flow-rate by 11%. The VAWT had a free running rotational speed of 479 rpm, power coefficient of 10.6%, and tip-speed-ratio of 1.88. [3].

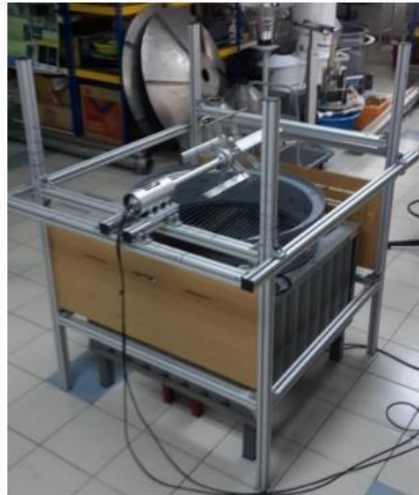


Figure 2.3.1: Complete scale model of VAWT on cooling tower.[3]

For the actual size of a cooling tower with a 2.4 m outlet diameter and powered by a 7.5 kW fan motor, it was estimated that a system with two VAWTs (side-by-side) can generate 1 kW of power which is equivalent to 13% of energy recovery[3].

2.4 Effect of the turbine radius, wind speed, shroud exit area to turbine area ratio and shroud exit length to the power generated and power coefficient.

As a whole unit to be optimize, a lot of design parameters need to take into account to obtain the optimum power output. Based on the research by Department of Mechanical Engineering and Materials Science, Washington University in St. Louis, USA in 2013, several set parameter of the shrouded wind turbine have been studied [4].

The schematic of the geometry of the configuration used in the computations is shown in Figure 2.4 Turbine radius (R_t), wind speed (V_o), shroud exit area to turbine area ratio (R_e/R_t), and shroud exit length ($L2_{max}$) are the key parameters that were varied to determine C_p and generated power for shrouded wind turbines. The shroud shape was optimized using a genetic algorithm (GA). Thirteen optimization cases were computed by varying various parameters which are summarized in Table 2.4.1.

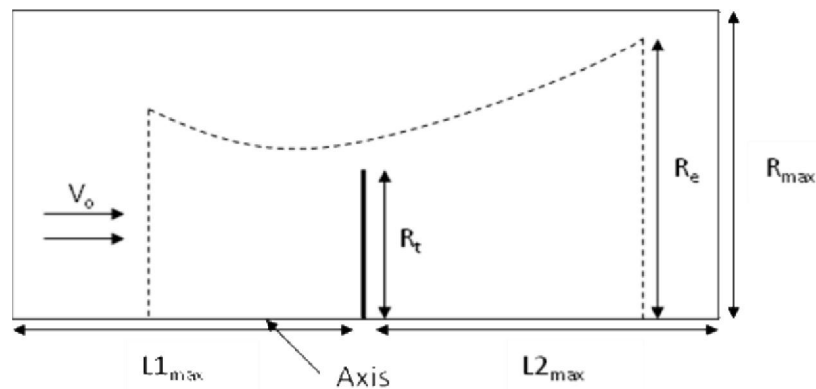


Figure 2.4.1: Schematic of axisymmetric HAWT actuator disk model and shroud parameters.[4]

Table 2.4.1: Parameters of thirteen computed cases. [4]

Case #	R _t (ft)				V _o (m/s)		R _e /R _t			L2max/R _t		
	1.5	5.0	8.0	10.0	5.71	7.0	2.0	2.56	3.0	1.0	2.0	3.0
1a		X			X			X		X		
1b		X				X		X		X		
1c		X			X		X				X	
1d		X			X				X			X
1e		X			X				X		X	
1f		X			X				X	X		
1g		X			X		X			X		
2a			X		X			X		X		
2b			X			X		X		X		
3a	X				X			X		X		
3b	X					X		X		X		
4a				X	X		X				X	
4b				X		X	X				X	

In this section, first describe the optimized shroud shape and solution obtained for case 1(a) of Table 2.4.1. Following the procedure outlined in Figure 2.4.1, first an adaptive structured mesh was generated using GAMBIT. The mesh inside the optimal shroud shape with the actuator disk is shown in Figure 1.5. Note that only half of the domain about the centre line of the diffuser is shown because of symmetry. Figure 2.4.2 (b) shows the total pressure distribution upstream and downstream of the actuator disk; it clearly shows the discontinuity in the total pressure across the actuator disk as expected.

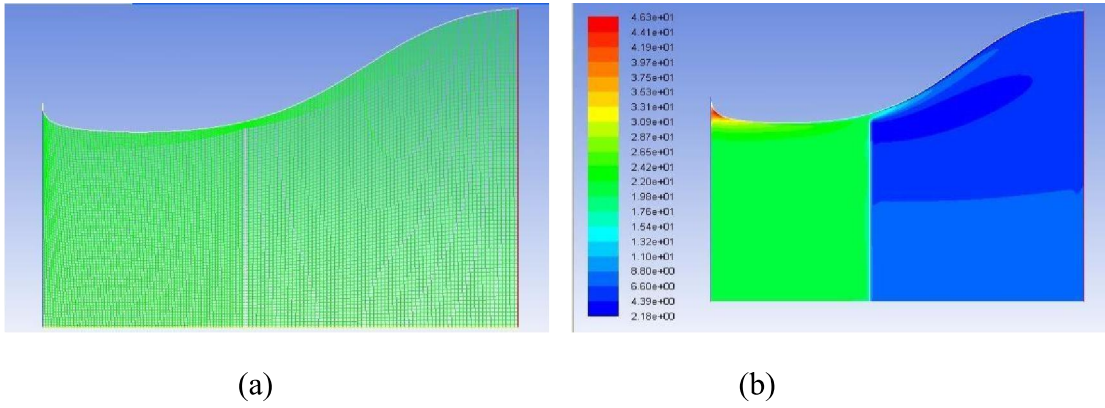


Figure 2.4.2: (a) Mesh inside the shroud for case 1(a). (b) Total pressure inside the shroud for case 1(a).

Figures 2.4.3 (a) and (b) respectively show the static pressure distribution and the velocity magnitude contours inside the shroud for case 1(a) of Table 2.4.1.

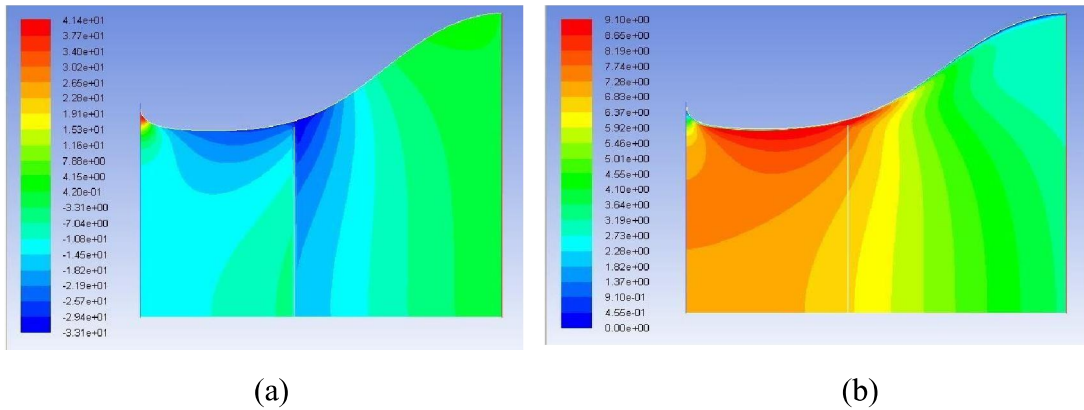


Figure 2.4.3: (a) Static pressure contours inside the shroud for case 1(a). (b) Velocity magnitude contours shroud for case 1(a).

Figures 2.4.4 (a) and (b) respectively show the variation in velocity and the change in static pressure distribution along the axis of the shroud for case 1(a) of Table 2.4.1. Figure 2.4.8 shows the change in the total pressure along the axis of the shroud. Figures 2.4.4 (b) and Figure 2.4.5 clearly show the jump in both the static pressure and total pressure across the actuator disk.

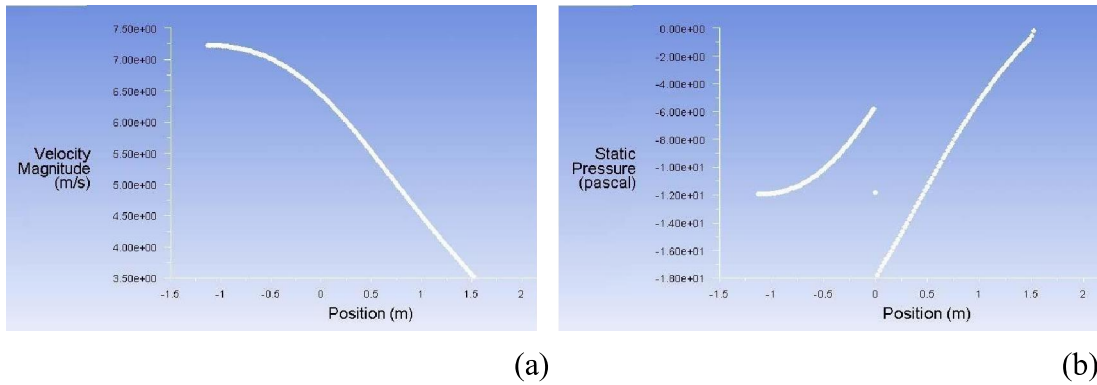


Figure 2.4.4: (a) Velocity variation along the centre variation along the line of axis the shroud for case 1(a). (b) Static pressure of the shroud for case 1(a). [4]

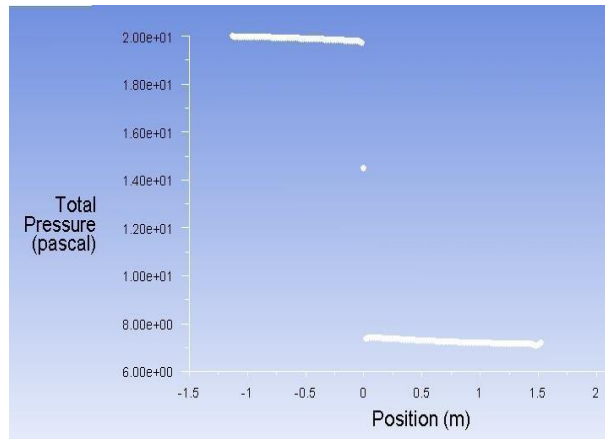


Figure 2.4.5: Total pressure variation along the axis of the shroud for case 1(a). [4]

Figure 2.4.6 shows the optimized shroud shapes obtained for maximum C_p for the thirteen cases whose parameters are given in Table 2.4.1. Table 2.4.2 gives the power production data and C_p for the thirteen optimized shroud cases.

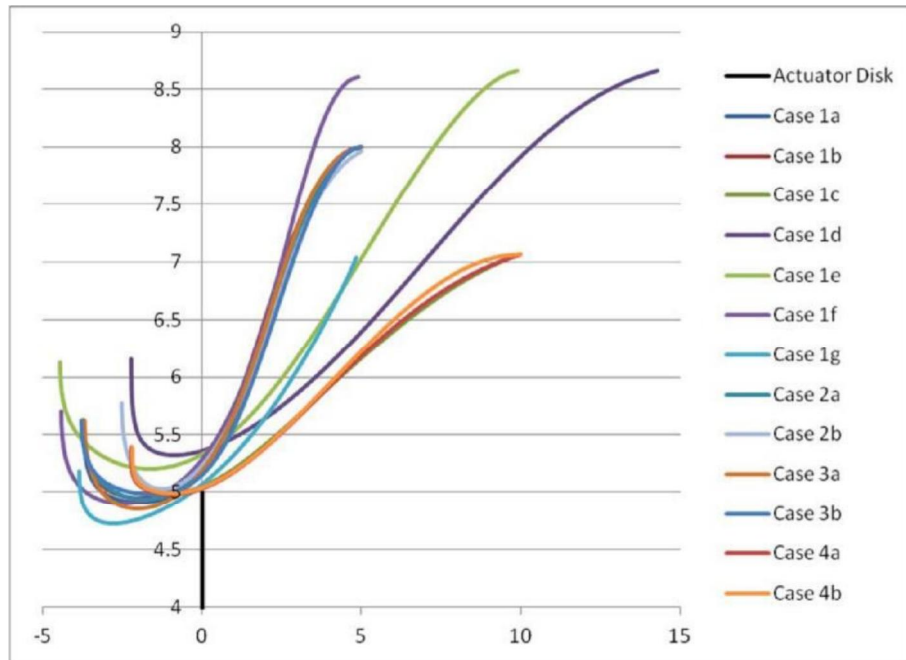


Figure 2.4.6.: Thirteen optimized diffuser shapes for thirteen cases in Table 1 for a 5 ft radius turbine (shown as an actuator disk).[4]

Table 2.4.2.: Power production and power coefficient C_p for thirteen cases of 1(a).[4]

Case	Power (W)	C_p
1a	717	0.86
1b	1294	0.84
1c	642	0.77
1d	889	1.07
1e	861	1.03
1f	755	0.91
1g	582	0.70
2a	1849	0.87
2b	3321	0.85
3a	65	0.87
3b	117	0.85
4a	2540	0.76
4b	4637	0.76

From the above result, we can see that the 1d, 1e and 1f configuration produce the highest power coefficient. This configuration can be used as reference for conceptual design modelling as initial design before the optimization can be done.

CHAPTER 3

METHODOLOGY

3.1 Design of Energy Harvester Unit

In this section, multiple design configuration of the air duct has been carried out to obtain the most effective air duct for the energy harvester unit as well as an electric generator unit to convert the kinetic energy into electrical energy. Air duct unit has been divided into four (4) sections which is curve duct, nozzle, diffuser and generator.

3.1.1 Design of Curve Duct

Curve duct design is a necessary to channel the air flow direction from horizontal flow to vertical flow in this case is upwards. This is due to the original exhaust air outlet flow in industrial site is in horizontal flow. However, there is limitation in term of space such as width, length and the height of the room. Curve duct design is depends on the input design parameter of the duct as listed below:

1. Cross-sectional area (A)
2. Turning Radius (R)
3. Particle path line (S)
4. Cross-sectional geometry

Cross-sectional area of the circle area obtained from he relationship

$$A = \pi r^2 \text{-----}(3.1)$$

Particle path line, S were calculated by

$$S = r\angle \text{-----} (3.2)$$

Where \angle is the angle between two radius.

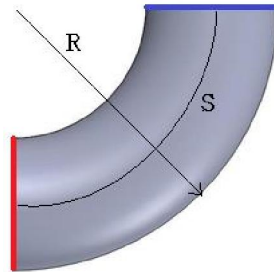


Figure 3.1.1.1 : The turning radius and particle path line indicator.

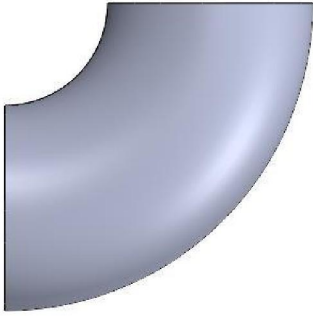
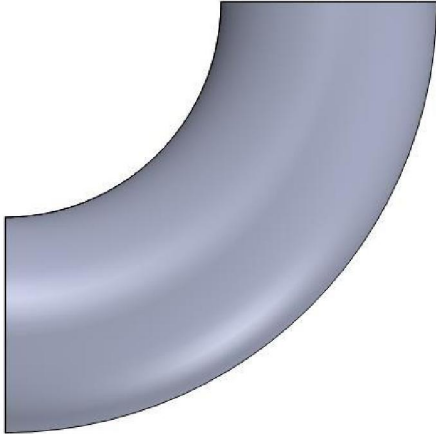
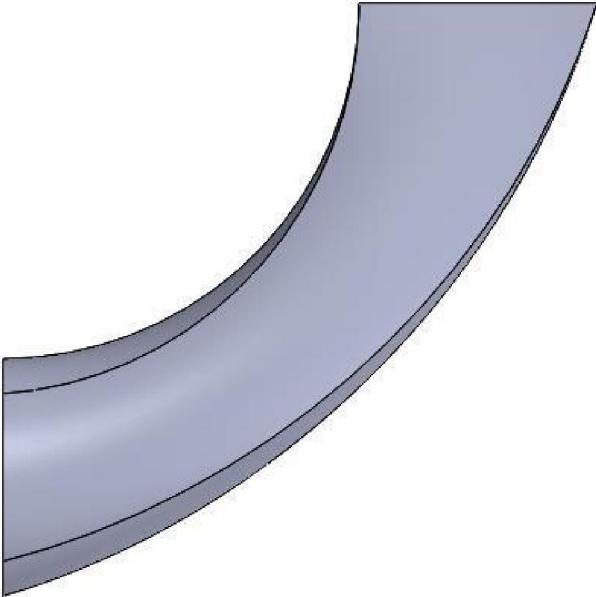
Table 3.1.1.1: Various design configuration of the curve duct.

Design\Parameter	Cross-sectional Area (A), m^2	Turning Radius (R), m	Particle Path Line (S), m	Outlet Cross-Sectional Shape
A	1.561	0.715 (R)	0.562	Circular
B	1.561	1.410 (2R)	1.107	Circular
C	1.561	2.115 (3R)	1.661	Circular
D	1.561	2.115 (3R)	1.661	Square

The cross-sectional area used is $1.561 m^2$ due to the exhaust fan outlet size used in Penfabric Mill 2. The turning radius and particle path line studied are based on the ratio 1:1, 1:2, and 1: 3..

Table 3.1.1.2: Design model of the curve duct with different parameters configuration.

Design	
A	<p>A 3D perspective rendering of a quarter-circle duct, showing its curved surface and the quarter-circle cross-section.</p>

B	
C	
D	

As for the design selection, numerical simulation have been executed by using computational fluid dynamic software called ANSYS Fluent. The simulation result are stated in the chapter 4.

3.1.2 Design of Nozzle and Diffuser

Nozzle and diffuser is an additional feature of air duct to increase the air velocity. The higher air velocity give produce higher kinetic energy to be harvest from the air flow. There are few ducts with different design configuration have been made and simulated through ANSYS to get the desired air flow velocity. The nozzle and diffuser design variation consist of the convergence ratio, divergence ratio and with or without the neck. The parameters guide of the nozzle and diffuser are as shown in Figure 3.1.2.1.

The nozzle and diffuser design parameter are as listed below.

1. Nozzle inlet cross-sectional area (A_1).
2. Nozzle outlet cross-sectional area (A_2).
3. Nozzle length (L_1).
4. Neck length (L_2).
5. Diffuser inlet cross-sectional area (A_3).
6. Diffuser outlet cross-sectional area (A_4).
7. Diffuser length (L_3).

The same area relationship was used as in (3.1).

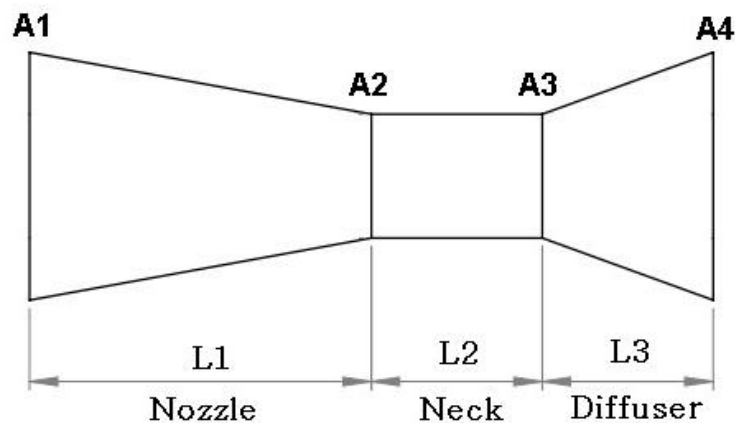



Figure 3.1.2.1: Parameter guide of the nozzle and diffuser.

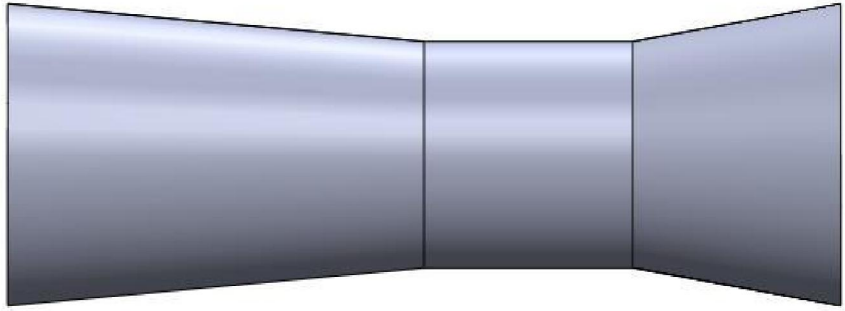
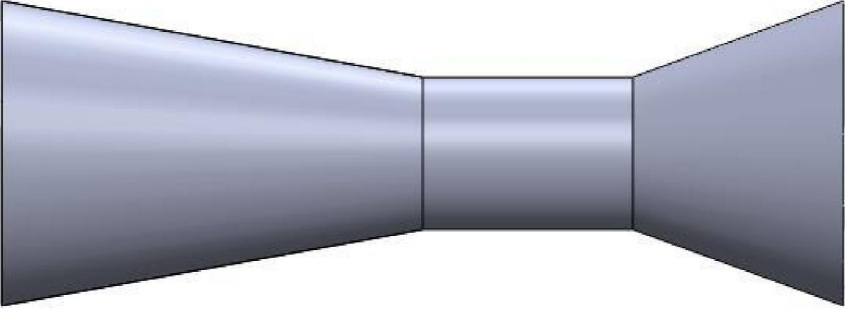
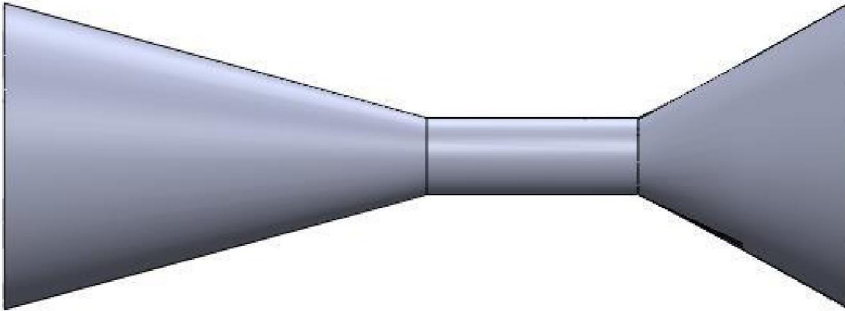
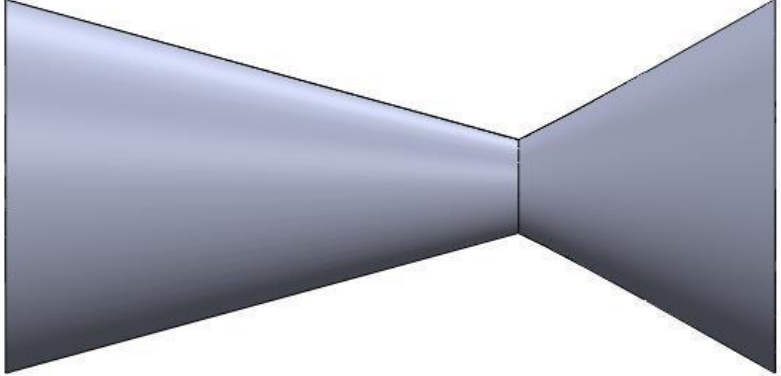
Table 3.1.2.1: Design parameter of the various nozzle and diffuser configuration.

Parameter \ Design	Nozzle inlet crosssectional area (A_1)	Nozzle outlet crosssectional area (A_2)	Nozzle length (L_1)	Neck length (L_2)	Diffuser inlet (A_3)	Diffuser outlet (A_4)	Diffuser length (L_3)
A	1.561	1.561	2	0	1.561	1.561	2
B	1.561	0.866	2	1	0.866	1.561	1
C	1.561	0.390	2	1	0.390	1.561	1
D	1.561	0.008	2	1	0.008	1.561	1
E	1.561	0.390	2	0	0.390	1.561	1

The nozzle and diffuser configuration have been done by diameter reduction ratio. For design A, there is no convergence design with diameter ratio and 1.0 while for design B,C and D reduction ratio of 0.75, 0.5 and 0.25 from the initial diameter are used. Table 3.1.2.1 show the calculated value of dimension used and have been illustrated via Solidworks models in Table 3.1.2.2.

Table 3.1.2.2: Design models of the nozzle and diffuser with different parameters configuration.

Design	
A	

B	
C	
D	
E	

3.1.3 Design of Generator Unit

Every wind turbine must have generator as one of its components. Generator is needed to convert the kinetic energy into electrical energy. The kinetic energy are harvested from the exhaust air flow that flow through the wind turbine and rotate the wind turbine. The power of the wind energy can be calculated using formula

$$P_w = \frac{1}{2} \rho A v^3 \text{-----}(3.3)$$

Where ρ is density of air, A is the cross-sectional area of the duct, and v is the wind velocity.

However, According to Betz's law, no turbine can capture more than 59.3% of the kinetic energy in wind. The factor 0.593 is known as Betz's coefficient. Practical utility-scale wind turbines achieve at peak 75% to 80% of the Betz limit [5].

The wind power in term of watt can be converted into mechanical horsepower (HP) by using the relation of,

$$1HP = 745.7 \text{ watt} \text{-----}(3.4)$$

The common parameter used involving rotational part like wind turbine is torque. From the wind turbine speed and wind power, we can get the useful torque value of the model by using equation,

$$(3.5) \quad \text{Torque} = \frac{\text{Power} \times 9550}{\text{turbine speed}} \text{-----}$$

Where torque unit is in Newton metre (Nm), power in horsepower (HP) and turbine speed in revolution per minute (rpm).

3.1.3.1 Wind Turbine Blade

Turbine blade is the crucial part of the wind turbine. Most wind turbines designed for the production of electricity consist of a two or three bladed propeller rotating around a horizontal axis. Wind turbine blades are designed to convert wind energy into usable shaft power called torque. Wind turbine blades work by generating lift due to their curved shape [7]. The side with the most curve generates low air pressure while high pressure air beneath pushes on the other side of the blade shaped aerofoil.

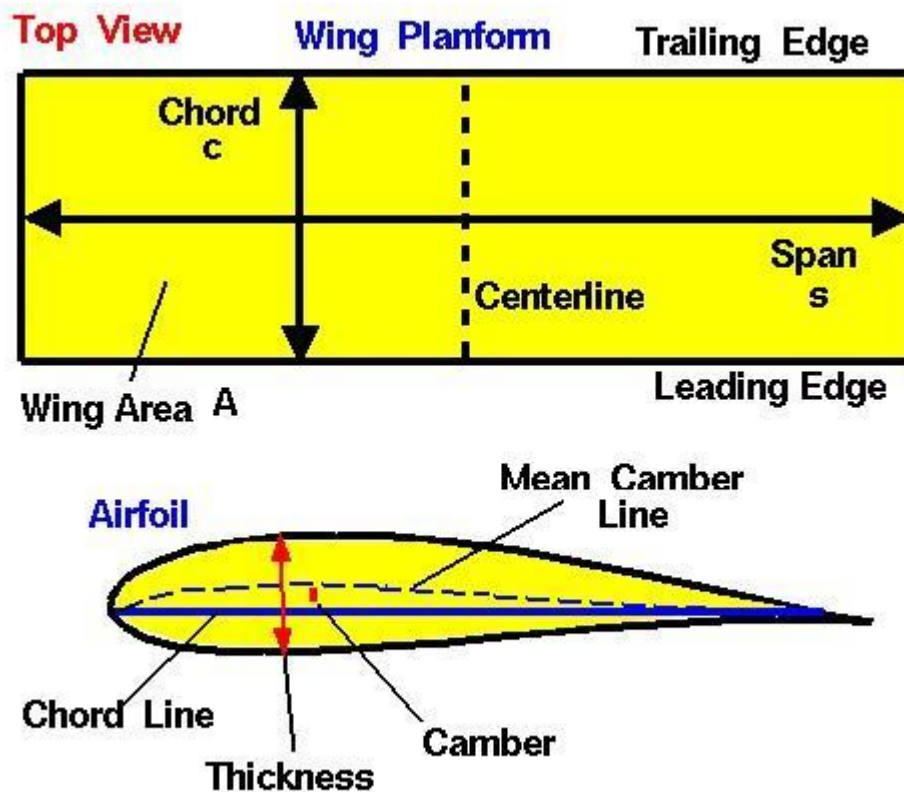


Figure 3.1.3.1.1.: Parameter guide of an airfoil .[9]

The turbine blade efficiency is highly depend on it airfoil configuration. The configurations consist of length of the chord line, blade thickness, mean chamber line span length and wing area as shown in Figure 3.1.3.1.1.

NACA 4412 - NACA 4412 airfoil

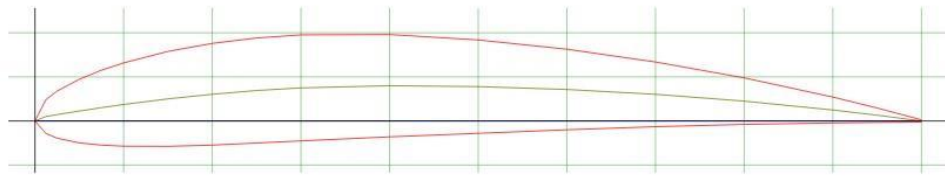


Figure 3.1.3.1.2: Cross-sectional design of NACA 4412 airfoil based on the coordinated grid .[10]

Maximum thickness is 12% at 30% chord and maximum camber at 40% chord. Based on the graph shown in Figure 3.1.3.1.3, the maximum lift coefficient is 1.45 at 0.07 drag coefficient.

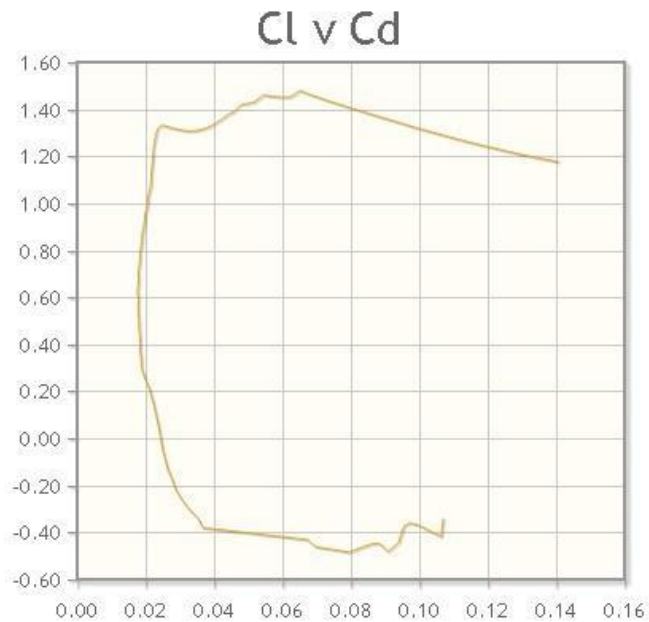


Figure 3.1.3.1.3: C_L relationship of NACA 4412 .[10]
 C_D

From the graph shown in Figure 3.1.3.1.4, the maximum lift coefficient of 1.45 is achieved at 14° angle of attack.

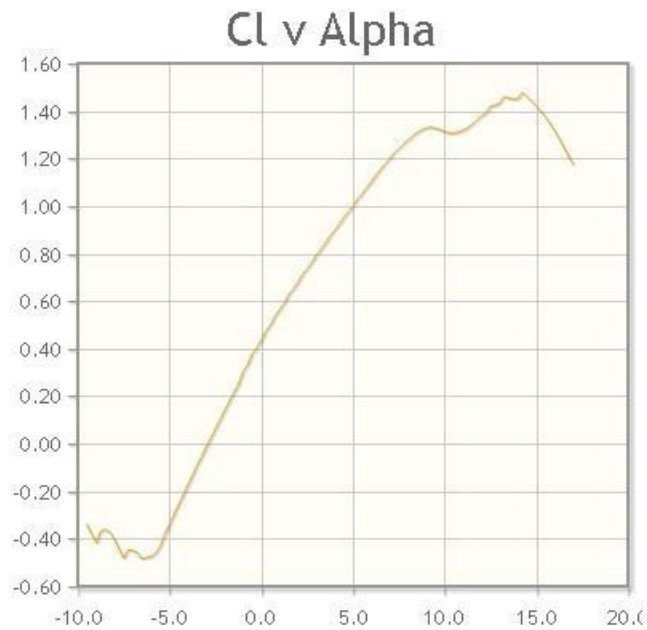


Figure 3.1.3.1.4: Lift coefficient against angle of attack of NACA 4412.[10]

Table 3.1.3.1.1.: Design parameter for NACA4412.

Parameter	Design Value
Angle of Attack	8.5°
Lift Coefficient	1.34
Drag Coefficient	0.022
Ratio between lift and drag coefficient	56.1

Three bladed rotor was considered for its aerodynamic and structural stability. NACA 4412 airfoil was used in this design. From the available performance data of 1 meter chord of airfoil NACA 4412, at Reynolds number of 100 000, the maximum $C_{L/D}$ is 56.1 at an angle of attack, $\alpha = 8.5^\circ$. The design parameter for NACA4412 was chosen as shown in Table 3.1.3.1.1.

3.2 Numerical Simulation of Air Duct

A computational fluid dynamics (CFD) tool, ANSYS Fluent software was used in this study. The numerical simulations were done over the three dimensional air duct structure. ANSYS Fluent software contain the broad, physical modelling capabilities needed to model flow, turbulence, heat transfer and reactions for industrial applications [6].

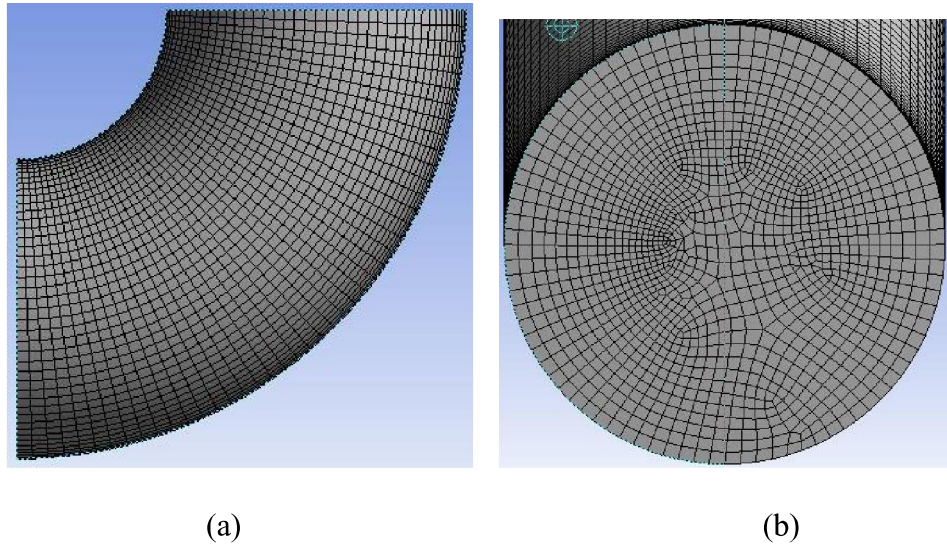


Figure 3.2.1(a): Side view of the structured mesh grid of curve duct design B with 1.41 m of turning radius. (b): structured mesh grid of the duct inlet.

Mesh cell type for 3D simulation is depend on the shape and geometry of the test component. For this project which only consist of common geometry such as cylindrical, cone and cuboid, hexahedron 3D cell type meshing have been used as shown in Figure 3.2.1(a) and 3.2.1(b). Element size were set at only 0.05m which is about 3.2% of the cross sectional size of the duct. The meshing result on the design B curve duct show it consist of 64 395 nodes and 61248 elements.

Pressure based type solver is used for the whole simulation set under transient time. For the viscous model, standard k-epsilon two equation was used with energy and radiation mode were not activated. The boundary conditions were set with inlet velocity at 18 m/s and initial gauge pressure at 0 Pascal same as the industrial exhaust fan outlet air velocity.

The numerical simulation of various design configuration of every section have been made as shown in Table 3.1.1.1 and Table 3.1.2.1. The simulation results of every